Soft Matter

# Direct Measurement of Interaction Forces between Charged Multilamellar Vesicles



| | |
|---|---|
| Journal: | *Soft Matter* |
| Manuscript ID: | SM-ART-11-2013-052785.R1 |
| Article Type: | Paper |
| Date Submitted by the Author: | 16-Jul-2014 |
| Complete List of Authors: | Frostad, John; University of California, Santa Berbara, Chemical Engineering<br>Seth, Mansi; University of California, Santa Barbara, Chemical Engineering<br>Bernasek, Sebastian; University of California, Santa Barbara, Chemical Engineering<br>Leal, L. Gary; University of California at Santa Barbara, Chemical Engineering |
| | |

# Direct Measurement of Interaction Forces between Charged Multilamellar Vesicles

*John M. Frostad, Mansi Seth, Sebastian M. Bernasek, and L. Gary Leal*

*Department of Chemical engineering, University of California, Santa Barbara*

ABSTRACT: Depletion-attraction induced adhesion of two giant (~50 μm), charged multilamellar vesicles is studied using a new Cantilevered-Capillary Force Apparatus, developed in this laboratory. The specific goal of this work is to investigate the role of dynamics in the adhesion and de-adhesion processes when the vesicles come together or are pulled apart at a constant velocity. Hydrodynamic effects are found to play an important role in the adhesion and separation of vesicles at the velocities that are studied. Specifically, a period of hydrodynamically controlled drainage of the thin film between vesicles is observed prior to adhesion, and it is shown that the force required to separate a pair of tensed, adhering vesicles increases with increasing separation velocity and membrane tension. It is also shown that the work done to separate the vesicles increases with separation velocity, but exhibits a maximum as the membrane tension is varied.

## 1 INTRODUCTION

Vesicles and vesicle suspensions are of interest in producing many industrial and consumer products like paint and fabric softener, and they also act as a simple model for advancing scientific understanding of some biological systems. The stability of vesicles in a suspension against phase separation depends on many different properties such as lamellarity, membrane tension and moduli, surfactant composition and chemical structure, solution composition, and temperature. One way that a vesicle suspension can be destabilized, via creaming or sedimentation, is for the vesicles to adhere to one another, thus forming larger, multi-vesicle "particles" that can overcome the stabilizing effect of Brownian motion. In this context, the interaction force between vesicles is of key importance and measurements of vesicle-vesicle adhesion are critical in assessing the potential of a particular vesicle suspension to exhibit this type of phase-separation induced instability. As enumerated below, there have been a number of studies aimed at measurements of the adhesion force under equilibrium conditions [1-6]. However, given that such suspensions are often subject to various types of flow, it is also important to investigate vesicle adhesion and de-adhesion under dynamic conditions which is the focus of the present study.

Specifically, we focus on the interactions of a pair of cationic vesicles suspended in a salt ($CaCl_2$) solution containing a small concentration of polymer, which produces a depletion attraction. In a recent study [7] the Surface Forces Apparatus (SFA) was used to measure the equilibrium (or thermodynamic) interaction force between a pair of cationic lipid bilayers, but

supported on a solid substrate, in a system that is otherwise very similar to that studied here[1]. It was found that depletion attraction [8] due to a small concentration of polymer in the suspending fluid can be sufficient to overcome the electrostatic repulsion between the charged bilayers, and thus produce a weakly attractive net force, albeit one with a strength of $O(kT)$ that would normally be assumed to be too weak to yield a stable doublet (the first step in destabilizing a suspension of vesicles made from one type of bilayer). However, the physics of the interaction between a pair of supported bilayers can be very different from the interaction between vesicles in a suspension, not only due to the dynamic effects mentioned above, but also because the bilayers of a vesicle are not supported and are therefore rather easily deformed. It is well-known that deformation contributes to an enhancement of the adhesive energy between a pair of surfaces and this has recently been the subject of a detailed theoretical study for vesicles [9].

It is also desirable to experimentally study the adhesive interaction between vesicles. Numerous experimental studies have focused on the adhesive interactions between giant vesicles under static or quasi-static (equilibrium) conditions. For example, Evans and co-workers developed a micro-pipette based method that enabled them to study vesicle-vesicle and vesicle-surface adhesion mechanisms [1,2] and also measure the adhesion energy per unit area of interaction for giant lipid vesicles adhering due to Van der Waals [3] and depletion attraction forces [4,5]. Brochard-Wyart and de Gennes developed a theory to predict the force required to separate a vesicle, held by suction on a micropipette, from a surface [10] under quasi-steady conditions (including some weak dynamic effects). More recently, Colbert *et. al* used a micropipette based force transducer to directly measure the force as a function of the radius of the adhesion zone of a neutral lipid vesicle on a gold-coated surface [6] and were able to verify the functional relationship between these two quantities predicted by Brochard-Wyart and de Gennes for quasi-static conditions [10]. Their study was the first to use a force transducer to directly measure adhesion forces (as opposed to the prior indirect determination of force via measurements of adhesion energy) between a vesicle and a surface.

On the other hand, investigations of the adhesive interactions under dynamic conditions, which are needed to complete the understanding of vesicle suspensions, are very few in number. One study that does address dynamics effects is the work of Chatkaew *et. al*. [11] who studied de-adhesion of a vesicle from a rigid surface under dynamic conditions. They used reflective

[1] The SFA study (7) examines cationic diC18:0 DEEDMAC surfactant bilayers which have fully saturated hydrocarbon tails, while the cationic diC18:1 DEEDMAC bilayers employed in the present study possess one unsaturation on each hydrocarbon tail which renders them in the 'fluid' state at room temperature. The surfactants are otherwise identical, having the same quaternary ammonium head-group, similar surface charge densities, and hence similar electrostatic interactions.

interference interaction microscopy to observe the thickness of the film between the vesicle and a surface while applying a constant force via an axisymmetric flow. However, recent work by Murrell et al. [12] shows that the dynamics of vesicle spreading during adhesion is qualitatively different for deformable versus rigid surfaces, and this suggests that it will be difficult to relate a study of the interaction of a vesicle and a rigid surface to the interaction of two vesicles.

The present work uses a new instrument called a Cantilevered-Capillary Force Apparatus (CCFA) [13] that enables direct force measurements between two vesicles at approach and separation velocities that are sufficient to expose dynamic (non-equilibrium) effects on adhesion/de-adhesion. This is a first step toward understanding the interactions of vesicles in suspension that is undergoing a flow. In the CCFA system, the vesicles are held at the ends of a pair of capillaries that can be moved toward one another or separated at a constant velocity. After a period of hydrodynamic resistance to approaching contact, the charged vesicles adhere to one another as a result of polymer induced depletion-attraction. The basic question is to understand the role of dynamics and deformability in both the adhesion and de-adhesion process. To study this, we consider a range of approach and separation velocities as well as membrane tensions.

The conditions in this study are such that the charged vesicles adhere to one another in the "strong adhesion" regime [9]. In this regime, the dimensionless adhesion energy per unit area, $w \equiv \left(\left|W_{ad}\right| R^2\right) / k_c$ is much greater than 1, indicating that bending energy plays a negligible role in determining the shape of the adhering vesicle [14]. Here, $W_{ad}$ is the (equilibrium) adhesion energy per unit area, $k_c$ is the bending modulus of the surfactant bilayer and $R$ is the radius of the undeformed vesicle. For a system comparable to the one under study $W_{ad}$ has been measured in the SFA to be -0.083 mJ/m$^2$ [7], whereas $k_c$ has been measured using micropipette aspiration to be $7\,k_BT$ [16]. For a vesicle having a radius of 40 μm, which is a typical value in these experiments, $w \sim O\left(10^6\right)$, verifying that the system lies in the strong adhesion regime.

To the authors' knowledge these are the first reported force measurements between two vesicles, under dynamic conditions. The measurements will be used to calculate the force of adhesion and the work (or energy) of adhesion under dynamic conditions. As a check for consistency, the experimental values will be compared to the SFA measurements of Anderson et al. [7] of the equilibrium force between supported bilayers of a surfactant which, as noted earlier, is similar to that used in this study. The values will also be compared with the theoretical predictions of Ramachandran et al. [9]. Conceptually, Ramachandran *et al.* predict that the deformability of vesicles (as compared to supported bilayers) has a very strong enhancing effect on the work of adhesion. The increased work of adhesion implies that deformability can substantially decrease the stability of vesicle suspensions.

# 2 MATERIALS AND METHODS

## 2.1 Description of the Instrument

The Cantilevered-Capillary Force Apparatus (CCFA) consists of two glass capillaries that are arranged such that the openings of the capillaries are axisymmetric as shown in Figure 1 (see also Figure 2). One capillary tube has been bent into an L shape to form a cantilever that acts as a force transducer. The motion of the cantilevered capillary is monitored by tracking the position of a laser beam that is reflected off of a mirror at the end of the cantilever. The second capillary, referred to as the "rigid capillary", is straight and can be moved forward and backward to bring the openings of the two capillaries closer together or farther apart with a resolution of about 5 nm. Both capillaries are connected to water reservoirs whose heights are manipulated to provide outflow or suction through the capillaries as needed. The suction pressure is used to pickup and hold vesicles at the tips of the capillaries. The rigid capillary used in this study had an outer diameter of 360 μm, while the capillary used to make the cantilever had an outer diameter of 150 μm. Both capillaries (New Objective, Woburn, MA) had an inner diameter of 20 μm and the cantilever had a spring constant of 46.9 ± 0.1 mN/m. The resolution of the interaction force that can be detected is about 1 nN in the present work. A full description of the instrument can be found in a separate paper [13].

In the CCFA the motion of the cantilever is well described by the equation for a driven harmonic oscillator:

$$m_{eff}\ddot{x} + b_d\dot{x} + kx = F(t). \quad (1)$$

Here $x(t)$ is the deflection of the tip of the cantilever, $m_{eff}$ is its effective mass, $b_d$ is the hydrodynamic drag coefficient for the cantilever, $k$ is the spring constant, and $F(t)$ is the sum of all the forces exerted on the cantilever during an experiment. When two vesicles are being separated from adhesive contact, the force $F(t)$ is made up of the DLVO (electrostatic and Van der Waals) force $F_{DLVO}$, the depletion attraction force $F_{DA}$, and hydrodynamic forces $F_H$:

$$F(t) = F_{DLVO} + F_{DA} + F_H. \quad (2)$$

The importance of the contributions of inertia ($m_{eff}\ddot{x}$) and drag ($b_d\dot{x}$) of the cantilever relative to the restoring force of the spring or Hooke's law ($kx$) can be evaluated by dimensional analysis:

$$C_{inertia} \equiv \frac{m_{eff}}{kt_c^2}; \quad C_{drag} \equiv \frac{b_d}{kt_c}. \quad (3)$$

Here $t_c$ is the characteristic time scale of the motion of the cantilever. The motion of the cantilever is proportional to the force and so it can be seen in Figure 3b that the motion of the capillary during separation of the vesicles is completed in ~1 second. In the present experiments the values of $C_{inertia}$ and $C_{drag}$ are $O\left(10^{-4}\right)$ and $O\left(10^{-2}\right)$ respectively. This means that the signal from the CCFA is well approximated by only the Hooke's law component of equation (1) and the drag and inertial components of the harmonic oscillator are negligible. Therefore equation (1) can be rewritten as:

$$kx(t) = F_{DLVO} + F_{DA} + F_H . \quad (4)$$

## 2.2 Giant Vesicle Preparation

Giant multilamellar vesicles were prepared by gentle hydration [15] from di(tallow ethyl ester)dimethyl ammonium chloride (diC18:1 DEEDMAC) surfactant, which was provided by Procter & Gamble (Cincinnati, OH) and is similar to the surfactant studied in the SFA experiments of Anderson et al. [7]. The cationic surfactant was dissolved in chloroform and then deposited on a glass surface through the evaporation of the chloroform subphase. The resultant film was allowed to dry for 24 hours in a vacuum desiccator. The surfactant layers were then hydrated at room temperature with a 300 mM sucrose solution. The hydrated solution was left unagitated for 24 hours while the giant vesicles formed. Giant vesicles visible by optical microscopy ranged in size from 20 – 100 μm in diameter. The number of bilayers in each giant vesicle varied from unilamellar to highly multilamellar with an onion-like internal structure. The latter type of vesicle was used in this study because of their relative robustness which was needed to stand up to the velocities and forces applied in the experiments. Adhesion measurements were attempted with numerous multilamellar vesicles but due to the difficulty of obtaining two well-behaved vesicles of approximately equal size, nearly all of the adhesion measurements reported here were performed on the same two vesicles. All solutions were prepared with Milli-Q water and contained 4.5 mM $CaCl_2$. Solutions were adjusted to a pH of 3.0 by the addition of concentrated HCl. Under these solution conditions, the bending modulus and stretching modulus of the individual bilayers were measured to be $7\,k_BT$ and 100 mJ/m$^2$ respectively [16].

## 2.3 Experimental Setup

Giant vesicles were transferred to the CCFA, which contained a 298 mM glucose solution with 4 wt.% of polyallylamine hydrochloride (PAH – Avg. MW = 15,000 gm/mol, Sigma Aldrich, St. Louis, MO) having a viscosity of 4.2 cP and a specific gravity of 1.0287. The slightly higher density of the sucrose solution inside the vesicles compared to the suspending solution containing glucose is highly convenient because it causes the vesicles to sink to the bottom of the CCFA chamber where they can be picked up by the cantilevered capillary. To

prevent nucleation of air bubbles on the capillaries during force measurements the polymer solution was degassed for 30 min prior to filling the CCFA chamber.

The CCFA chamber was cleaned with ethanol and DI water between experimental trials. Once clean, the chamber was filled with a solution containing small unilamellar vesicles in order to coat the charged glass surfaces of the chamber. The small unilamellar vesicles, being positively-charged, rupture on the negatively charged glass forming a bilayer on the surface [17]. This prevents the giant multilamellar vesicles which are also positively charged, from adhering to the glass and ensures a reproducible mechanical response of the vesicles when they are held at the tips of the capillaries [16]. Both capillaries were left under suction for 15 min to coat the internal glass surfaces. The chamber was then thoroughly rinsed with water before the chamber was filled with glucose solution containing polymer and then sealed. Giant vesicles were injected into the chamber via an access port on the top surface.

## 2.4 Experimental Procedure

To measure the interaction between two vesicles, a single vesicle needs to be held on the end of each capillary by suction. Vesicles were obtained from the bottom surface of the chamber by rotating the cantilevered capillary until the tip was oriented downwards at a 45° angle relative to the bottom surface. With the capillary angled downwards toward the lower surface it was positioned near a vesicle and a sufficient suction pressure was applied to lift the vesicle from the surface. After lifting the vesicle from the surface it was aligned with and then transferred to the rigid capillary by the application of positive and negative gauge pressures to the cantilevered and fixed capillaries, respectively. By the same technique, a second vesicle of approximately the same size was picked up to be held on the cantilevered capillary. The cantilevered capillary was then carefully rotated so that the tip of the capillary was horizontal again without damaging the vesicle and the two capillaries were aligned in an axisymmetric configuration as shown in the inset to Figure 1. Image-processing software and hardware-automation software written in MATLAB were used to measure the vesicle radii and perform the experiments.

In each experimental trial the vesicles are first pushed together by moving the rigid capillary forward at a constant velocity, then allowed some time to equilibrate without further motion, and finally separated by moving the rigid capillary backward at a constant velocity. The range of velocities used in this study is between 10 μm/s and 100 μm/s which falls into the low Reynolds number regime ($\mathrm{Re} = 0.005 - 0.05$ based upon the length scale of the tip of the cantilever (see Figure 2), ~2 mm, and $\mathrm{Re} = 0.2\times10^{-3} - 2\times10^{-3}$ based upon the diameter of the vesicles ~80 μm).

# 3 RESULTS AND DISCUSSION

## 3.1 Typical Force Curve

This section begins with the description of a complete measured force curve for one representative experimental trial, shown in Figure , for which the velocity of the capillary in both the forward and reverse directions was 30 μm/s. Images of the vesicles at a few key points during the experiment are shown in Figure a for reference. The video from which these images are taken is provided in the supplemental material, and the onion-like structure and dynamic behavior of the vesicles can be seen more clearly in the video than in the still images. Note that both vesicles in this representative case have additional surfactant bilayer/vesicles stuck to the outside (i.e. the less structured mass behind the vesicle on the right) that are sufficiently far away from the contact zone that they appear to have minimal or no impact on the adhesion experiments.

In the first image in Figure a, the vesicles are not moving and the interaction force is expected to be zero. In Figure b there are two important observations to make regarding the force measured between 0 and 1 second. First, there is a high frequency oscillation in the measurement; this corresponds to electrical noise (± ~4 mV) from the data acquisition card (National Instruments USB 6009, Austin, TX). Second, there is a slow drift upwards in the signal even though there is not yet any motion of the capillaries; this is an example of the effect of random thermal fluctuations. This level of drift in the signal is estimated based on calculations of the thermal expansion of the lever arm which supports the rigid capillary to be the result of a temperature change of around 0.1 degrees Celsius. The effects of thermal fluctuations are generally small $O(1-2\ \mathrm{nN})$ and average out to zero over several trials. Care was taken to reduce thermal fluctuations in the lab as much as possible.

Between image 1 and image 2 the vesicles are moving together with a corresponding hydrodynamic interaction. The force measured during this phase of the interaction provides a check for consistency by making a comparison with theory. During this initial phase of approach where the deformation of the vesicles is very small, their interaction should be well represented by the known hydrodynamic interaction of two rigid (non-deforming) spheres. According to the exact hydrodynamic solution for two spheres approaching at a constant velocity [18], the drag force should exceed 1 nN when the separation distance between the spheres is less than ~7 μm and 2 nN for a distance less than 2.5 μm [18]. As expected, the magnitude of the predicted force is consistent with the measured force at these separation distances as determined from approximate measurements of the separation distance from the images. As the vesicles are pushed closer together, the force between the vesicles will eventually become large enough to deform the vesicles, resulting in a flattened zone in the region of closest approach due to the hydrodynamic (lubrication) pressure in the thin film. Once the vesicles are deformed, the theory for non-deforming spheres is no longer applicable and a theoretical solution for the interaction force is not available for comparison.

The second image shows the vesicles under compression with the hydrodynamically deformed region in the middle, but prior to adhesion due to depletion attraction. It was not possible to accurately control the exact magnitude of the compressive force in each experiment, but in all of the data presented in this work the vesicles are moved together far enough to result in a small positive compressive force. During the period (~4.5 – 5.5 seconds) just after the motion of the rigid capillary is stopped, the thin film of fluid between the vesicles is undergoing "drainage", in which fluid is pushed out of the film by the difference between the lubrication pressure in the thin film generated by the compressive force pushing the vesicles toward each other, and the ambient pressure in the surrounding fluid. When two vesicles collide in a flow, this drainage process is a critical factor in determining whether the vesicles adhere, and has been the subject of two recent theoretical studies in this group [19 and the references therein, 20].

Image 3 shows the vesicles after the film of fluid has drained sufficiently to allow depletion attraction effects to overcome electrostatic and hydrodynamic forces, and an adhesive contact zone has formed. The formation of an adhesive contact zone can be clearly observed in the video (see supplemental material) as an abrupt change of shape in the contact zone. This is usually accompanied by a visual increase in the radius of the flattened region between the vesicles and a corresponding decrease in the compressive force as seen in the force curve in Figure  at about 5.5 seconds. We note, in plotting the radius of the flattened region in Figure  that a distinction is drawn between the flattened region produced by hydrodynamic forces prior to adhesion and the radius of the adhesion zone. The radius of the adhesion zone $R_c$ reflects the radius of the flattened contact region at the instant that depletion attraction is triggered and is considered to be zero prior to this in spite of the flattening due to hydrodynamic forces. Once the depletion attraction is triggered and the vesicles can adhere, the radius of the adhesion zone is observed to increase over time to a steady value as shown by the solid dots in Figure b. The radius of the adhesion zone is measured using an image analysis algorithm in which the edges of the adhesion zone are manually pinpointed in each image using a computer mouse (again, note that the adhesion zone is much more readily discerned in the original video images than is suggested by the reproduced images in Figure ). The steady value of the radius of the adhesion zone would be equal to the *equilibrium* contact radius $R_{c,eq}$ if the force between the vesicles were exactly equal to zero when it is measured. However, there is a small compressive force between the vesicles when the radius of contact reaches a steady value; nevertheless, within the measurement resolution (1 – 2 μm) the steady value of the radius of the adhesion zone is approximately equal to the true equilibrium contact radius. This can be seen most easily by noting that there is no measurable change in $R_c$ when the force passes through zero during the separation process. For this reason, the steady value of the radius of the adhesion zone is assumed to be equal to $R_{c,eq}$ in the remainder of the paper.

For the present system wherein the vesicles are adhering in the strong adhesion regime, the radius of the contact region [14] at equilibrium is related to the tension in the membrane and the energy of adhesion per unit area by the Young equation as [8,10]:

$$\left|W_{ad}\right| = \tau\left(1 - \cos\theta_E\right). \tag{5}$$

Here $W_{ad}$ is the adhesion energy per unit area, $\tau$ is the membrane tension, and $\theta_E$ is the equilibrium contact angle. For two vesicles of the same radius $R$ the equilibrium contact angle can be inferred from the equilibrium contact radius $R_{c,eq}$ [21]:

$$\sin\theta_E = \frac{R_{c,eq}}{R}. \tag{6}$$

Substituting equation (6) into equation (5), the energy of adhesion per unit area can now be written as:

$$\left|W_{ad}\right| = \tau\left(1 - \sqrt{1 - \left(\frac{R_{c,eq}}{R}\right)^2}\right). \tag{7}$$

Note that for polymer-induced depletion attraction between cationic vesicles, the value of $W_{ad}$ is determined by the solution conditions, i.e. the salt and polymer concentration and the radius of gyration of the polymer [9]. In all of the experiments the salt and polymer concentration, and hence the value of $W_{ad}$ were held fixed; though the exact value of $W_{ad}$ is not known. According to equation (7) for constant $W_{ad}$, an increase in the equilibrium contact radius implies a decrease in the membrane tension i.e. there exists an inverse relationship between the equilibrium contact radius and the membrane tension. This inverse relationship was evident when the initial membrane tension prior to adhesion was changed by varying the suction pressure on the vesicles. As the suction pressure and therefore initial membrane tension was increased, the radius of the equilibrium adhesion contact zone was found to decrease in accordance with equation (7), and this has also been shown in previous studies that employed suction pressure to hold vesicles onto pipettes in order to study vesicle-vesicle adhesion [21, 22, 23].

The fourth image in Figure a shows the vesicles adhering during separation. As the vesicles are pulled apart, the contact radius of the adhesion zone decreases over time, a process termed “peeling”, and the measured force becomes negative. When the force is strong enough to overcome the sum of the hydrodynamic and adhesion forces acting on the vesicles, the vesicles separate completely and the force exerted on the cantilever rapidly relaxes back to zero as shown in image 5. The magnitude of this force to overcome adhesion is referred to in this work as the force of adhesion, which as already noted, includes both hydrodynamic and non-hydrodynamic

contributions. Although the vesicles completely separate in this sample experiment, there are also cases where instead of separating, one of the vesicles undergoes a shape instability and a thin tether is formed between the vesicles (see Figure ). This occurs when the tension in the vesicle is not high enough to support the force required to overcome the adhesion and has been observed and studied by other authors [11, 24]. Only cases where complete separation occurs are used for the data in this paper.

As mentioned earlier, the data presented in Figure represents one specific case at a given velocity and membrane tension. In the next sub-section, many such measurements are used to show the magnitude of the force of adhesion for a range of tensions at a fixed velocity and for a range of velocities at a fixed initial membrane tension. Note that the value of the tension is dependent on the amount of area dilation in the membrane and therefore may be a function of time during adhesion and separation of the vesicles. Therefore, it is the initial value of the tension that is varied/held constant between trials. In the following sub-section, we also present the work of adhesion calculated from the same set of force measurements. Recall that the terms "force of adhesion" and "work of adhesion" in this paper refer to the total quantities including both hydrodynamic and non-hydrodynamic contributions.

Before proceeding, a few caveats concerning the present system are briefly mentioned. As discussed previously, the exact value of $W_{ad}$ is not known though it could, in principle, be calculated from theory as was done by Anderson et al. [7]. However, for the system they studied (which is very similar to the one considered here) the theory is not in good agreement with the experimental results from the SFA experiments. Hence, $W_{ad}$ is viewed as unknown, meaning that equation (7) cannot be used in the present work to calculate the membrane tension. The membrane tension could also be calculated from the length of the vesicle sucked into the capillary and the suction pressure. This method was not used in the current experiments because the experimental apparatus was not set up to measure suction pressure. Note, however, that the lack of this information does not affect the interpretation of the results described below.

### *3.2 Force of Adhesion*

The force of adhesion is taken to be the magnitude of the minimum in the force curve during separation of the vesicles (i.e. ~7 nN in Figure b). Using this metric, the force of adhesion is plotted in Figure 5a as a function of the velocity of the rigid capillary. The error bars on the data correspond to the noise in the force measured over a period of two seconds immediately prior to each adhesion measurement. The scatter in the data is due to minor differences in the membrane tension and (primarily) random thermal fluctuations that cause shifts in the zero point of the measurement as described previously. The key points from Figure 5a are that the force varies between approximately 5-9 nN, and increases with increasing velocity – rapidly at low velocities and more gradually at higher velocities. A nonzero force at $V = 0$ corresponds to the equilibrium value (in the absence of dynamic effects) of the adhesive force. Unfortunately, this value could

not be obtained in the present experiments because thermal drift is of the same order of magnitude as the measurement at very slow velocities.

Recall that the measured force is a sum of the DLVO (electrostatic and Van der Waals) force $F_{DLVO}$, the depletion attraction force $F_{DA}$, and hydrodynamic forces $F_H$ (see equation (4)) at the moment when the two vesicles separate. Though there are a number of factors that may contribute to the velocity dependence of the measured force of adhesion, any velocity dependence of $F_{DLVO}$ and $F_{DA}$ is weak[2] and the increase in the measured force with increase of velocity is due to the velocity dependence of the hydrodynamic force as discussed below.

If two vesicles are in physical contact, i.e. without a film of fluid separating them [10], the vesicles can be pulled apart by the process of peeling in which the radius of contact $R_c$ decreases. In the present case, the short range electrostatic repulsion means that there will always be a thin fluid film separating the two vesicles. Nevertheless, the peeling mechanism can still occur. In this case, the film radius decreases with time, but the thickness of the film remains (approximately) fixed. The hydrodynamic contribution to the measured force is then due to viscous dissipation emanating from the fluid motion caused by the receding motion of the contact radius, which will increase as the separation velocity increases.

With a thin film present, there is also the possibility of separating the vesicles by a process referred to here as "pulling" in which the film thickness near the line of centers, increases with time[3]. If the vesicles were truncated spheres of fixed shape with a flat disk-like region of radius $R_c$ between them, then the hydrodynamic contribution to the force can be calculated analytically [26]. There are two factors that will cause significant deviations from this well-described case. First, the vesicles are deformable. It is known from prior studies of drops [25], but is also intuitively obvious that deformation will decrease the hydrodynamic force required to pull the

[2] The DLVO (electrostatic and Van der Waals) force $F_{DLVO}$ can be rate dependent due to charge regulation effects as previously noted by Anderson et al. (7). These authors show that the measured forces between cationic bilayers in the SFA under dynamic (non quasi-static) conditions are more repulsive than predicted by the equilibrium DLVO theory and this effect increases at higher velocities. Additionally, it is also possible that the contribution due to depletion attraction $F_{DA}$ may also depend on the rate of separation, due to limitations in the rate of mass transfer of the polymer into or out of the thin film. However, no theory for depletion attraction accounts for this and we believe that it is likely to be a minor effect in the present system.

[3] This would, in fact, be the only possible mechanism if the vesicles were not deformable.

vesicles apart, and this effect will increase with the separation velocity. Second, the contact area also decreases due to peeling, and the area that remains at the moment that the vesicles separate may also depend on the velocity. An example of this for the case of two drops being pulled apart can be found in ref [25].

While there is no exact expression for the two distinct contributions to the hydrodynamic force (i.e. from peeling and pulling, respectively) due to the dynamically changing shape of the vesicles, the order of magnitude of the two contributions can be estimated. First, the contribution due to peeling is expected to scale as [11]:

$$F_{peeling} \sim \frac{\mu R_c^2}{b_0}\frac{dR_c}{dt}. \qquad (8)$$

Here, $\mu$ is the viscosity of the suspending fluid, **Error! Objects cannot be created from editing field codes.** is the equilibrium film thickness of the adhered vesicles, and $R_c$ is the contact radius as before. It is assumed that the initial thin film separation $b_0$ is 5 nm based upon the fact that it is below the radius of gyration of the polymer and approximately equal to the equilibrium separation distance between the adhered vesicles as calculated from the theory [9]. Taking typical values of $R_c$ from the experiments and assuming that the scaling constant is $O(1)$, equation (8) gives an initial value at the onset of peeling (i.e. when $R_c$ takes it's equilibrium value) of approximately 2 nN. However, this force decreases rapidly as $R_c$ is decreased by the peeling process. Indeed, the data for $R_c$, as well as the argument given below, suggests that $R_c$ may be as small as a few hundred nanometers at the moment when the vesicles pull apart, and it seems clear that the peeling force cannot contribute significantly to the measured adhesion force.

The order of magnitude of the hydrodynamic force for separation in the pulling mode is dominated by the lubrication pressure in the thin film between vesicles, which is sensitive to the shape and radius of the thin film, and the separation velocity $db/dt$. However, the shape of the thin film of fluid between the vesicles cannot be experimentally evaluated accurately enough with the current setup to allow it to be incorporated into a scaling argument. Instead we provide a crude estimate for the lubrication pressure in the film, assuming that it is bounded by a pair of parallel disks of radius $R^*$ and separation $b(t)$. The calculation of the lubrication pressure for this "model" and integration to get the force is straightforward and the result is well-known from lubrication theory [26]:

$$F_{Pulling}(t) = \frac{3\pi\mu R^{*4}}{2b(t)^3}\frac{db}{dt}. \qquad (9)$$

For rigid vesicles the velocity of separation $db/dt$ could be computed from the experimental separation velocity $V$ and the deflection of the cantilever $x$:

$$V = \frac{dx}{dt} + \frac{db}{dt} \quad \rightarrow \text{where} \qquad x(t) = Vt + x_0 + b_0 - b(t). \tag{10}$$

In fact, if the deflection of the cantilever is neglected and it is assumed that $db/dt = V$, the force that would be required to separate the vesicles via this pulling mode, assuming that $R^* = R_{c,\,eq}$ and $b(t) = b_0$, would be $O(1\ \text{N})$!, far in excess of the measured forces. However, it is evident from the data (cf. Figure 3) that the vesicles initially peel apart so that $R_c$ decreases with time. In fact, a simplistic picture of the process is that the force transmitted from the capillaries to the vesicles increases with time (and the vesicles acquire an elongated shape in order to transmit the forces from the point of adhesion to the micropipettes), and $R_c$ decreases until the pulling force just balances the sum of the depletion attraction, DLVO and hydrodynamic forces required to pull the vesicles apart. This is the measured adhesion force.

Equation (9) is used along with expressions for the depletion attraction force $F_{DA}$ and DLVO force $F_{DLVO}$ to numerically estimate the value of the adhesion force for this simplified model. The depletion attraction force is simply [8,9]:

$$F_{DA} = \frac{\pi R^{*2} W_{ad}}{R_g} \mathrm{H}\left(R_g - b\right), \tag{11}$$

where $R_g$ is the radius of gyration of the polymer and H represents the Heaviside function. Because the effect of the DLVO force is to effectively produce a strong repulsion at close separation, it was represented in the calculations by a simple Hookean repulsion, $k_1\left(b - b_0\right)\mathrm{H}\left(b_0 - b\right)$ with a large spring constant $k_1$, which is computationally much better behaved than the full theoretical expression. Since the available visual images do not provide sufficient resolution to determine $R_c$ at the moment of separation and its velocity dependence is unknown, the value of $R^*$ was taken to be a constant independent of $V$. As before, the initial thin film separation $b_0$ is assumed to be 5 nm.

Using equations (9), (10), and (11) in equation (4), the differential equation is numerically solved to compute an estimate for the effect of the pulling mechanism on the force of adhesion.

Although the vesicle is not rigid as assumed in equation (10), the assumption that it does not undergo any significant change in shape during the pulling process is likely quite reasonable, given that pulling only occurs for a brief period at the very end of the separation process.[4] In effect, $R^*$ is treated as a free parameter and a value is sought that gives an average force that is the same order of magnitude as the data. This yields $R^*$ ~320 nm. The resulting force versus velocity plot is shown in Figure 6. The main point of this plot is to demonstrate that the force associated with pulling can still be in the nN range that is measured at the very end of the peeling process where the contact radius can be seen from Figure 3 to be very small. In contrast, the force from peeling becomes much smaller as the contact radius is reduced (for $R^*$ ~320 nm, the peeling force estimated from equation 8 is only 0.4 pN). Furthermore, the shape of the hydrodynamic contribution is qualitatively similar to what is measured. This provides support for the hypothesis that the pulling mechanism is a significant part of the de-adhesion process. However, we do not suggest that the actual value of $R^*$ is 320 nm. The real film shape will not be a flat disk as assumed and value of $R^*$ will likely be a function of the separation velocity.

In Figure 5b the force of adhesion is plotted as a function of the equilibrium contact radius $R_{c,eq}$ divided by the equivalent radius $R = 2R_1R_2 / \left(R_1 + R_2\right)$ of the vesicles for a velocity of the rigid capillary equal to 30 μm/s. Recall that the equilibrium contact radius is inversely related to the membrane tension by equation (7). In the range of $R_{c,eq} / R$ between 0.4 and 0.5, the force of adhesion is approximately constant (independent of $R_{c,eq} / R$). This includes the value 0.44 studied in Figure 5a. For values of $R_{c,eq} / R$ greater than 0.5, however, it can be seen from the data that the force of adhesion decreases with decreasing membrane tension. It is known from the earlier work of Colbert et. al. [6] that the force of adhesion should decrease with decreasing membrane tension. We suggest that this may be due to the fact that the vesicles are more easily deformed.

As a final analysis of the measured force of adhesion, the results can be compared to the measurements of Anderson et al. [7] performed in the SFA. In their study the force of adhesion was measured between rigid DEEDMAC bilayers in 4.5 mM $CaCl_2$ solution with 4 wt% of polyallylamine. The force of adhesion measured in the SFA can be scaled, according to the Derjaguin approximation for two spheres, by the radius using the following equation [9]:

[4] This is confirmed by related numerical simulations being done as part of the PhD project of Martin Keh in our group.

$$F_{adhesion} = \pi R |W_{ad}| . \quad (12)$$

Using a value of -0.083 mJ/m$^2$ for $W_{ad}$ (from Anderson et al. [7]) and a radius of 39 μm gives ~10 nN. This value was measured in a quasi-static way such that dynamic effects are negligible. This can be compared to the force between deformable vesicles in the limit of zero velocity. From the data in the present experiments (Figure 5) it looks like this value would be on the order of 1 – 4 nN. It should be noted that in the measurements of Anderson et al. [7], the pH was 4.0 compared to 3.0 in the present experiments which would result in a more repulsive electrostatic force in the present system due to increased dissociation of the cationic DEEDMAC head groups at lower pH. The most we can say is that the two measured values are roughly of the same order of magnitude. In the work of Ramchandran et al. [9] the gradient of the energy of adhesion (i.e. the force of adhesion) is approximately the same (see Figure 3a in reference [9]) for non-deforming vesicles as for deforming vesicles suggesting that the force of adhesion is relatively insensitive to the effect of deformability under equilibrium conditions. The comparable order of magnitude between the measurements in the SFA and the CCFA may be taken as being consistent with this prediction.

### 3.3 Work of Adhesion

The effect of the velocity of the rigid capillary and the membrane tension on the total work of adhesion required to separate two adhering vesicles is also considered. This is important because in a mixing process, for example, the flow needs to be strong enough to pull the vesicles apart, but also the vesicles need to stay in a configuration in the flow long enough to perform the work needed to separate them. Otherwise, the vesicles may not separate during mixing even if the instantaneous force produced by the flow is larger than the force of adhesion.

In order to calculate the work of adhesion in this study, the measured force was integrated as a function of the change in the distance $\Delta L$ between the two cantilevers as they are separated (see the shaded area in Figure 7a). The force is integrated beginning when the force between the vesicles has reduced to zero during separation and ending at the point when separation occurs and a force "jump out" is observed. As seen in Figure 7b, the work of adhesion increases with velocity by $\sim 20 \times 10^6 k_B T$. Just as in the case of the separation force, a finite intercept is expected at $V = 0$, corresponding to the adhesive work in the absence of dynamic effects. The apparent linear dependence of the data suggests that the value at $V = 0$ can be deduced from a linear extrapolation of the data in 7b; this is estimated to be $\sim 20 \pm 5$ x $10^6 k_B T$. The error is estimated from the standard deviation in the data at a single velocity.

This extrapolated value of the work of adhesion can be compared to a theoretical prediction of the work required to separate two deformable vesicles under equilibrium conditions. Assuming constant vesicle volume[5], the theoretical value can be calculated according to [9]:

$$U = -4\pi R_{eq}^2 \left[ K_a \left( \frac{\left(3-\cos\theta_E\right)}{4^{1/3}\left(1+\cos\theta_E\right)^{1/3}\left(2-\cos\theta_E\right)^{2/3}} - 1 \right)^2 - |W_{ad}| \left( \frac{\left(1-\cos\theta_E\right)}{4^{1/3}\left(1+\cos\theta_E\right)^{1/3}\left(2-\cos\theta_E\right)^{2/3}} \right) \right]. \quad (13)$$

Here $K_a$ is the area expansion modulus of the vesicle bilayer which has been measured to be 100 mJ/m$^2$ for the DEEDMAC surfactant used in this study [16]. For an equilibrium energy of adhesion per unit area of -0.083 mJ/m$^2$ at 4 wt% of 15,000 MW poly(ally)amine having a radius of gyration $R_g = 7$ nm [27], the theoretical prediction for the work of adhesion of two vesicles of $R_{eq} = 39$ μm is $10\,\mathrm{x}\,10^6 k_B T$. This is within the same order of magnitude as the experimental result. This can also be compared to the work of adhesion measured between supported bilayers in the SFA by Anderson et al. [7]. In this case, the work of adhesion between supported bilayers is predicted to be much lower than the work for deformable bilayers. The work of adhesion measured in the SFA (scaling by the radius) is approximately $6\,\mathrm{x}\,10^3 k_B T$ which is three orders of magnitude lower than what is measured in the present work. Clearly the deformability of the vesicles has a very large impact on the work of adhesion as predicted by Ramachandran et al. [9].

Interestingly, as a final observation it was found that the measured work of adhesion is not monotonic as a function of the membrane tension, as shown in Figure 8b. The maximum observed in the work at $R_c / R_{eq} = 0.51$ can be qualitatively explained by the following hypothesis. The force required to separate the vesicles is finite at infinite tension ($R_c / R_{eq} = 0$) and decreases as the membrane tension decreases ($R_c / R_{eq}$ increases; see Figure 5b). Figure 8a shows the force as a function of stretching distance for three sample cases when $R_c / R_{eq} =$ 0.42, 0.51, and 0.63. The curves A and C have been shifted up and down by 10 nN for clarity. At the

[5] The constant volume assumption is valid when the Laplace pressure (which tends to drives water out of the vesicle) is much smaller than the osmotic pressure due to the presence of non-ionic and ionic species (which tends to prevent loss of water). The ratio of the two is ~ 0.01 in the present case, indicating that the assumption of constant vesicle volume is valid. For more details on Eq. 11 see reference 9.

same time, the deformability and therefore the degree to which the vesicles will be stretched during separation increases from 22 μm to 32 μm and 45 μm respectively. All three curves in Figure 8a have been shifted so that $\Delta L = 0$ when the force equals zero for ease of comparison. This increase in deformability effectively increases the range of integration of the force and therefore acts to increase the work done, while the decreasing magnitude of the force acts to decrease the work done. The two competing effects result in the non-monotonic dependence of the work on membrane tension seen in Figure 8b.

Finally, we note that for both the force of adhesion and the work of adhesion, the degree of lamellarity of the vesicles is expected to change the quantitative results because of the direct impact on the membrane tension. Other effects such as internal viscous dissipation may be expected as well, but a study of these effects may be pursued in future research efforts. There is also ample opportunity for developing quantitative theoretical explanations for the observed behavior of the vesicles in these experiments.

## 4 CONCLUSION

A Cantilevered-Capillary Force Apparatus has been used to directly measure the force and work of adhesion between two charged, giant multilamellar vesicles. To the authors' knowledge this is the first study of this kind. The measurements in the present work confirm that, as in quasi-static measurements, the membrane tension is a key parameter affecting force and work of adhesion during dynamic interactions. When the membrane tension is high enough to prevent tether formation (and allow separation), hydrodynamic effects make measurable contributions to the force and work of adhesion measured in this system. The results suggest that the lubrication force in the thin film between the vesicles at the final moments of de-adhesion dominates the hydrodynamic contribution to the total force. Because the lubrication force is rate dependent, a larger force will be required to separate two adhering vesicles pulled apart at a higher velocity. Although there is also expected to be a hydrodynamic contribution due to the peeling process, the impact on the measured force during separation is below the resolution of the instrument for these experiments, which is consistent with scaling estimates. On the other hand, it is observed here and in other studies that the force decreases with decreasing membrane tension, providing evidence that the proposed peeling mechanism may become increasingly important during de-adhesion at lower values of membrane tension.

Although the value of the membrane tension is important for determining the force of adhesion, it has a much stronger impact on the work of adhesion. For example, the present results provide experimental evidence to support the theoretical predictions of Ramachandran et al. [9] which state that while the *magnitude* of the force of adhesion changes little with varying membrane tension, the magnitude of the work of adhesion can change by orders of magnitude. Indeed, the work of adhesion measured here is 1000 times larger than that measured in the SFA

(where the tension is effectively infinite because the membranes are adhered to a solid substrate) for a similar system. Surprisingly, the measurements also reveal a non-monotonic relationship between the work of adhesion and the membrane tension that is hypothesized here to result from the combined effect of lower adhesion force and the higher global deformability with decreasing membrane tension.

## 5 ACKNOWLEDGEMENTS

The authors would like to thank the Institute for Multiscale-Materials Studies and the National Science Foundation for funding this project (NSF GOALI Grant # CBET-0968105), and Procter & Gamble for providing the DEEDMAC surfactant.

## 6 REFERENCES

1. Evans, E A. 1980. Analysis of adhesion of large vesicles to surfaces. Biophys. J. 31:425–431.

2. Evans, E. A. 1985. Detailed mechanics of membrane-membrane adhesion and separation. I. Continuum of Molecular Cross-bridges. Biophys. J. 48:175–183.

3. Evans, E., and M. Metcalfe. 1984. Free energy potential for aggregation of giant, neutral lipid bilayer vesicles by Van der Waals attraction. Biophys. J. 46:423–426.

4. Evans, E., and M. Metcalfe. 1984. Free energy potential for aggregation of mixed phosphatidylcholine/phosphatidylserine lipid vesicles in glucose polymer (dextran) solutions. Biophys. J. 45:715–720.

5. Evans, E., and D. Needham. 1988. Attraction between lipid bilayer membranes in concentrated solutions of nonadsorbing polymers: comparison of mean-field theory with measurements of adhesion energy. Macromolecules. 21:1822–1831.

6. Colbert, M-J., A N. Raegen, C. Fradin, and K. Dalnoki-Veress. 2009. Adhesion and membrane tension of single vesicles and living cells using a micropipette-based technique. Eur. Phys. J. E. 30:117–121.

7. Anderson, T.H., S.H. Donaldson, H. Zeng, and J.N. Israelachvili. 2010. Direct measurement of double-layer, Van der Waals, and polymer depletion attraction forces between supported cationic bilayers. Langmuir 26:14458–14465.

8. Israelachvili, J.N. 2010. Intermolecular and Surface Forces, Third Edition. Academic Press.

9. Ramachandran, A., T.H. Anderson, L.G. Leal, and J.N. Israelachvili. 2011. Adhesive interactions between vesicles in the strong adhesion limit. Langmuir: 27:59–73.

10. Brochard-Wyart, F. and P.G. de Gennes. 2003. Unbinding of adhesive vesicles. Comptes Rendus Physique 4:281–287.

11. Chatkaew, S., M. Georgelin, M. Jaeger, and M. Leonetti. 2009. Dynamics of vesicle unbinding under axisymmetric flow. Phys. Rev. Lett. 103:248103.

12. Murrell, M. P., Voituriex, R., Joanny, J., Nassoy, P., Sykes, C., Gardel, M.L. 2014 Liposome adhesion generates traction stress. Nat Phys 10, 163–169.

13. Frostad, J.M., M.C. Collins, L.G. Leal. 2013 Cantilevered-capillary force apparatus for measuring multiphase fluid interactions, *Langmuir,* **29,** 4715-4725.

14. Evans, E. 1991. Entropy-driven tension in vesicle membranes and unbinding of adherent vesicles. Langmuir 7:1900–1908.

15. Reeves, J.P., and R.M. Dowben. 1969. Formation and properties of thin-walled phospholipid vesicles. J. Cell. Physiol. 73:49–60.

16. Seth, M., A. Ramachandran, and L.G. Leal. 2013. Direct measurements of effect of counterion concentration on mechanical properties of cationic vesicles. Langmuir 29:14057-14065

17. Cremer, P.S., and S.G. Boxer. 1999. Formation and spreading lipid bilayers on planar glass supports. J. Phys. Chem. B. 103:2554-2559.

18. Brenner, H. 1961. The slow motion of a sphere through a viscous fluid towards a plane surface. Chem. Eng. Sci. 16:242–251.

19. Ramachandran, A., and L.G. Leal. 2010. A scaling theory for the hydrodynamic interaction between a pair of vesicles or capsules. Phys. Fluids. 22:091702–091702–4.

20. Frostad, J.M., J. Walter., and L.G. Leal. 2013. A physical constraint on the length scale of the pressure gradient for capillary pressure driven flow in thin fluid films, Physics of Fluids **25**, 052108

21. Sun, Y., C.C. Lee, and H.W. Huang. 2010. Adhesion and merging of lipid bilayers: a method for measuring the free energy of adhesion and hemifusion. Biophys. J. 100:987–995.

22. Evans, E., and D. Needham. 1987. Physical properties of surfactant bilayer membranes: thermal transitions, elasticity, rigidity, cohesion and colloidal interactions. J. Phys. Chem.

91:4219–4228.

23. Nam, J., and M.M. Santore. 2007. The adhesion kinetics of sticky vesicles in tension: the distinction between spreading and receptor binding. Langmuir. 23:10650–10660.

24. Waugh, R.E. 1982. Surface viscosity measurements from large bilayer vesicle tether formation II: experiments. Biophys. J. 38:29–37.

25. Yoon, Y., F. Baldessari, H.D. Ceniceros and L.G. Leal, 2007. Coalescence of Two Equal-sized Deformable Drops in an Axisymmetric Flow. Physics of Fluids, **19,** 102102.

26. Leal, L.G. 2007. Advanced Transport Phenomena: Fluid Mechanics and Convective Transport Processes. 1st ed. Cambridge University Press.

27. Jachimska, B., T. Jasiński, P. Warszyński, and Z. Adamczyk. 2010. Conformations of poly(allylamine hydrochloride) in electrolyte solutions: experimental measurements and theoretical modeling. Colloid Surface A 355:7–15.

# 7 FIGURE CAPTIONS

**Figure 1.** Schematic representation of the Cantilevered-Capillary Force Apparatus (CCFA). Two vesicles can be held at the tips of two capillaries as shown in the inset. A force exerted on the tip of the cantilevered capillary will cause a deflection that can be tracked using a laser reflected off a mirror attached near the end.

**Figure 2**. Schematic of the capillaries in the CCFA showing the notation used in the calculation of the lubrication force and the relative dimensions.

**Figure 3.** (a) Images from a vesicle adhesion experiment at distinct points in time. Note, a small amount of aggregated bilayer is stuck to the outside of the vesicle on the right, but remains outside of the adhesion and interaction zone throughout the experiment. (a1) Prior to moving together, (a2) compressed during thin film drainage, (a3) adhering due to depletion attraction, (a4) being stretched during separation, and (a5) after separation while they are still moving apart. The video of this experiment can be viewed in the supporting materials. (b) The solid line represents the force measured by the CCFA during a vesicle adhesion experiment when the position (dashed line) of one vesicle is moved forward until compressed against the second vesicle and then moved back to separate the vesicles after 5 seconds time for equilibration. The solid dots represent the radius of the adhesion zone between the two vesicles and the points in time that correspond to the images in (a) are labeled.

**Figure 4.** Example of vesicles that do not separate, but instead undergo a shape instability (center) and form a thin tether that remains attached to the second vesicle (right). No tether is present prior to adhesion (left).

**Figure 5.** (a) Force of adhesion as a function of velocity of the rigid capillary for $R_{c,eq} / R = 0.44 \pm 0.02$. (b) Force of adhesion as a function of $R_{c,eq} / R$ for a velocity of 30 μm/s. For both graphs $R = 39 \pm 1$ μm.

**Figure 6.** The calculated force of adhesion based upon a simplified model (equation (9)) in which the film between vesicles is modeled as a nondeforming flat disk with an assumed value for the radial extent of the disks of $R^* = 320$ nm. The circles represent the calculated force of adhesion while the triangles are produced using with the same calculation, but with the adhesion energy per unit are set to zero for comparison.

**Figure 7.** (a) Measured force as a function of the change in the distance between the tips of the capillaries where the compressed position is used as a zero-point reference. The shaded area corresponds to the work (hydrodynamic and non-hydrodynamic) required to separate the

vesicles. The number labels coincide with the images and labels in Figure 3. (b) Work of adhesion as a function of velocity for $R_c / R_{eq} = 0.44 \pm 0.02$ and $R_{eq} = 39 \pm 1$ μm.

**Figure 8.** (a) Measured force as a function of the change in the distance between the tips of the capillaries for $R_{c,eq} / R = 0.42$ (A), 0.51 (B), and 0.63 (C). The position when force = 0 is used as a reference for $\Delta L$ and curves A and C have been shifted up and down by 10 nN for clarity. The shaded area corresponds to the work required to separate the vesicles. (b) Work of adhesion as a function of $R_{c,eq} / R$ for a velocity of 30 μm/s and $R = 39 \pm 1$ μm. The labels A, B, and C correspond to the respective force curves in (a). Error in each data point are estimated to be ±5 nN based on the scatter in the data observed in Figure 7b.

# 8 FIGURES

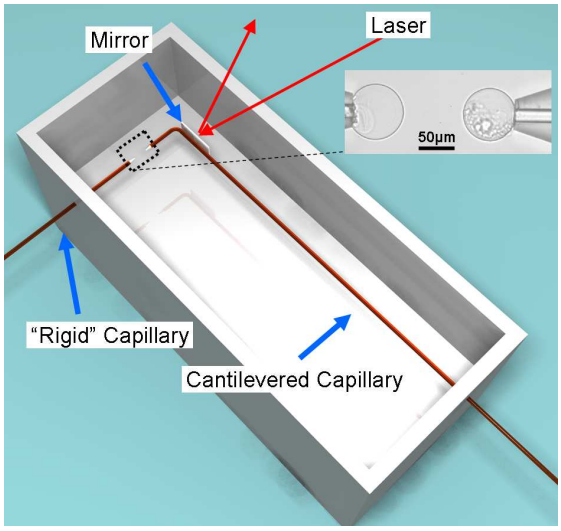


**Figure 1**

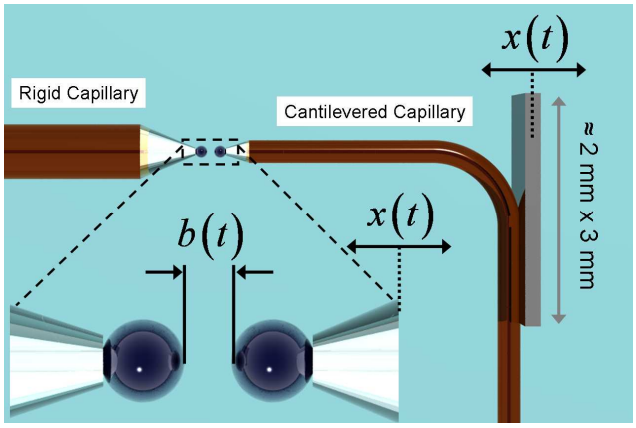


**Figure 2**

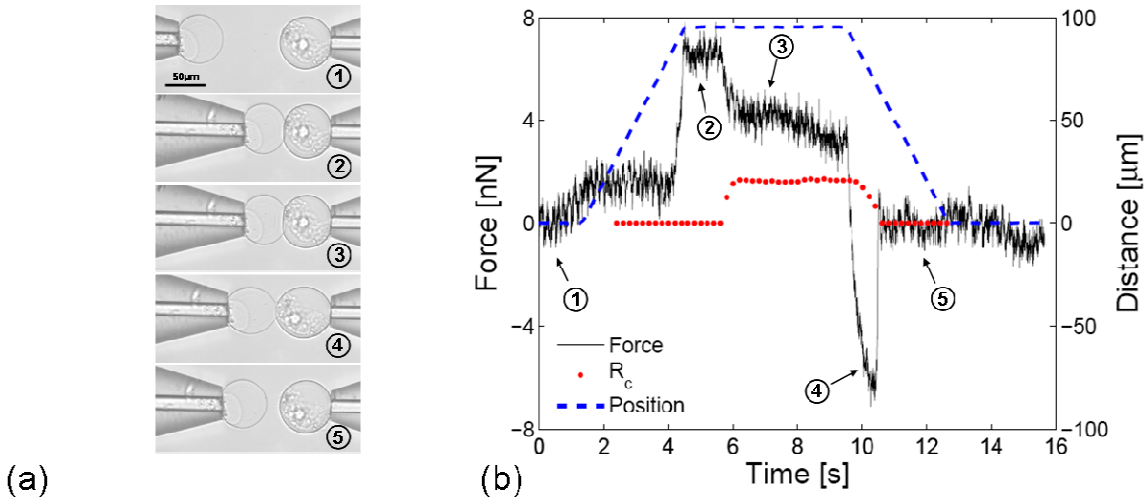


**Figure 3**

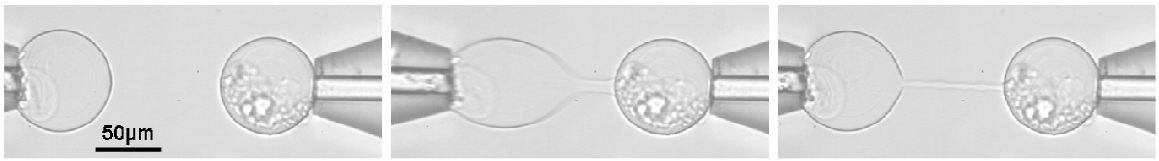


**Figure 4**

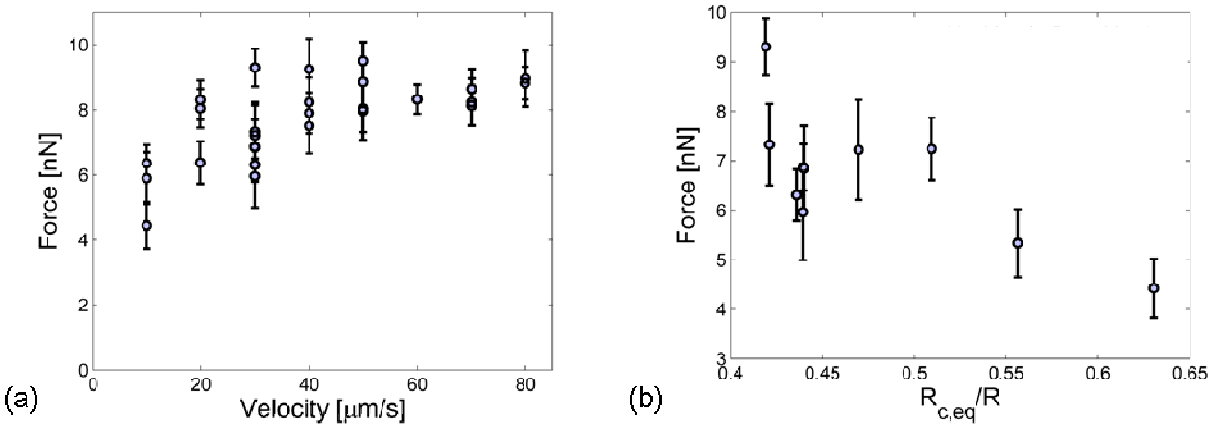
(a)
Force [nN]
Velocity [μm/s]
0
2
4
6
8
10
0
20
40
60
80
(b)
Force [nN]
$R_{c,eq}/R$
3
4
5
6
7
8
9
10
0.4
0.45
0.5
0.55
0.6
0.65

**Figure 5**

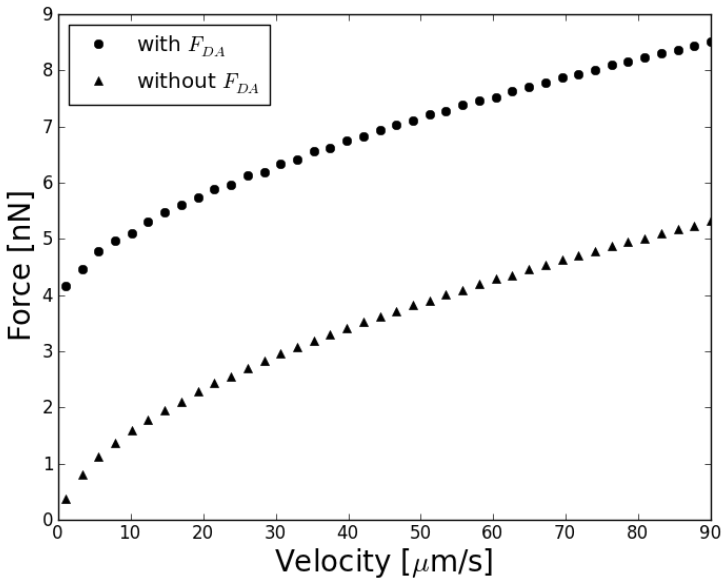
with $F_{DA}$
without $F_{DA}$
Force [nN]
Velocity [$\mu$m/s]
0
1
2
3
4
5
6
7
8
9
0
10
20
30
40
50
60
70
80
90

**Figure 6**

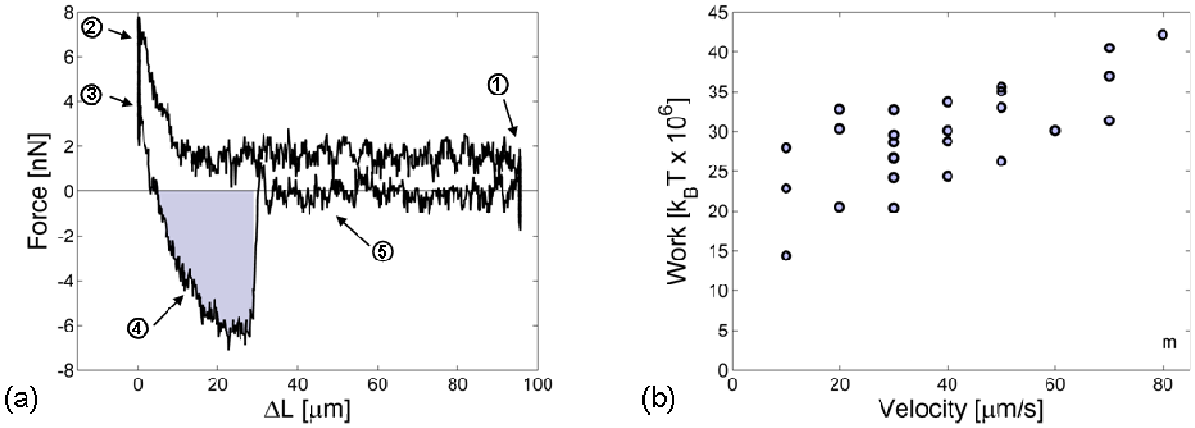


**Figure 7**

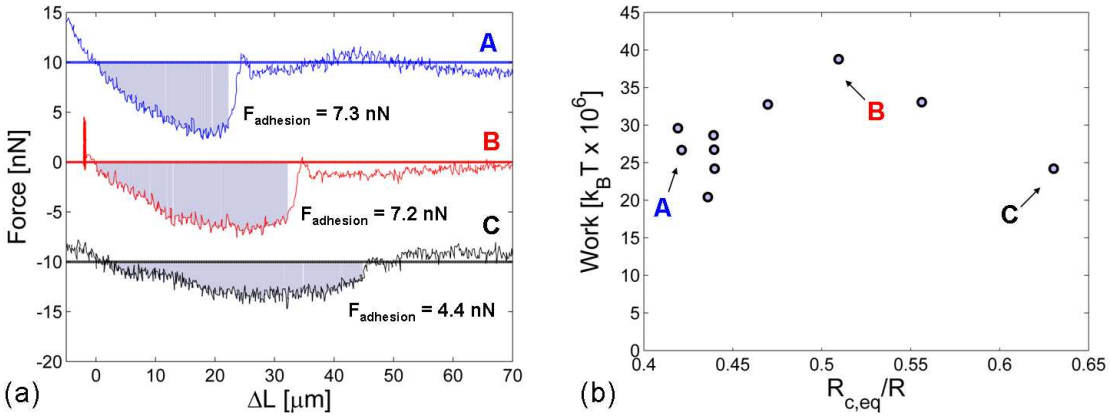
A
B
C
$F_{adhesion}$ = 7.3 nN
$F_{adhesion}$ = 7.2 nN
$F_{adhesion}$ = 4.4 nN
Force [nN]
ΔL [μm]
(a)
Work [$k_B$ T x $10^6$]
$R_{c,eq}$/R
(b)

**Figure 8**